# ULTRASONIC DETECTION OF WELD BEAD GEOMETRY

Nancy M. Carlson and John A. Johnson

Idaho National Engineering Laboratory
EG&G Idaho, Inc.
Idaho Falls, Idaho 83415

## INTRODUCTION

The three basic components needed to truly automate a welding machine are being investigated in a joint research effort involving the Idaho National Engineering Laboratory (INEL) and the Massachusetts Institute of Technology (MIT). These are: sensors to detect the physical properties of the weld, a model of the welding process, and a control system that can take signals from the sensors, for use in the feedback control, to the welder. Research programs at the INEL are developing electro-optic and ultrasonic sensors to detect the physical properties of the weld [1] and a model [2] of the welding process to relate these properties to parameters in the control model being developed at MIT. This paper discusses the ultrasonic sensing techniques which detect weld bead geometry on root passes during the gas metal arc (GMA) welding process and the approach for acquiring and evaluating the ultrasonic signal and assessing its quality for use as an input signal to a closed loop controlled welding system.

## PREVIOUS WORK

The feasibility work on detecting the molten weld pool started in 1977 [3]. Water was used as the coupling medium between the transducer and a 25.4 mm steel welding sample, which was only partially immersed in water to allow welding on upper surface. Stationary weld spots were formed using the gas tungsten arc (GTA) welding process. The weld pool was detected using 5 MHz immersion transducers generating longitudinal and mode-converted shear waves in the sample. A good correlation was found between the interfaces observed in the acquired longitudinal data and the temperature gradient field code for the solid-liquid interface, the top solid surface, and the top liquid surface.

The proof-of-principle for a weld inspection system was achieved with the concurrent inspection system that uses pattern recognition to detect flaws in the solidified weld bead in partially completed welds [4,5]. In the concurrent welding research, a transducer, mounted inside a liquid-filled tire, was positioned on the welding side of a sample to sense defects 330 mm behind the welding torch in the solidified weld metal. Analysis of the ultrasonic data collected during GTA cover passes showed that two type of flaws, lack of full side wall penetration and porosity, can be detected and can be reliably distinguished from each other and

differentiated from good weld using pattern-recognition techniques. An analysis code, the ray tracing field code, was developed to determine the sound path in the selected welding geometry to assure correct placement of the transducer.

## DETECTION OF MOLTEN WELD BEAD GEOMETRY

Based on the feasibility work with the detection of the molten pool and the experience gained acquiring ultrasonic data from the solidified weld metal during the welding process, research is now focused on detecting the molten weld pool geometry on the root pass. A computer-controlled data acquisition system and a video system are designed to acquire the data during GMA welding on a realistic weld sample. The wealth of ultrasonic signals acquired from the molten weld pool required a systematic approach to determining the origin of these signals. Machined samples were designed and fabricated to simulate the weld sample preparation prior to welding, the different molten weld pool geometries during welding, and the variation in solidified weld fill level after the weld pass. A correlation was made between the data acquired from the machined samples at ambient temperature and from the molten weld pool.

### Ultrasonic Data Acquisition System

The transducer used for the ultrasonic sensing of the weld bead geometry is a 5 MHz highly damped, broadband, 6.35 x 6.35 mm element transducer mounted on a lucite wedge that generates a 45° refracted shear ultrasonic beam in the carbon steel weld sample. The transducer and wedge were selected because a 45° refracted shear wave provides a favorable coefficient of reflection at the molten/solid interface and the distance from the sound entrance point to the front edge of the wedge allows positioning of the transducer close to the edge of the weld preparation for data collection. The transducer, operating in the pulse-echo mode, is housed in a metal fixture that is machined to provide a couplant reservoir, to protect the lucite wedge and transducer from the radiant heat of the arc, to promote motion down the weld sample, and to reduce wear on the wedge (Fig. 1).

A fixture was designed to allow the transducer to move along the plate parallel to the weld preparation in alignment with the torch. Data were acquired from a transducer positioned normal to the weld preparation 12 mm from the top corner and 27 mm from the bottom corner of the weld preparation. The transducer fixture is designed for mounting other transducers to obtain additional information during the welding process (Fig. 2).

Two methods are used to collect ultrasonic data from the molten weld pool. The first is a video system which includes a camera, monitor, and a video recorder to record the real-time ultrasonic signals displayed on the oscilloscope screen. The video system provides a convenient method for the research team to review a welding run. The second data acquisition method uses a computer-controlled data acquisition system to digitize and to store the amplified ultrasonic signal [6]. The computer communicates with modules in a CAMAC crate via the CAMAC dataway. Several of the modules perform control functions during data acquisition. A transient digitizer digitizes the amplified signal from the transducer at 32 MHz (a data point every 31.25 ns) under the control of a timing generator (Fig. 3).

The data acquisition software records a digitized A scan of the voltage output displayed on the oscilloscope. As the welding torch moves, driven by an encoder mounted on the side beam welder, data are collected at intervals

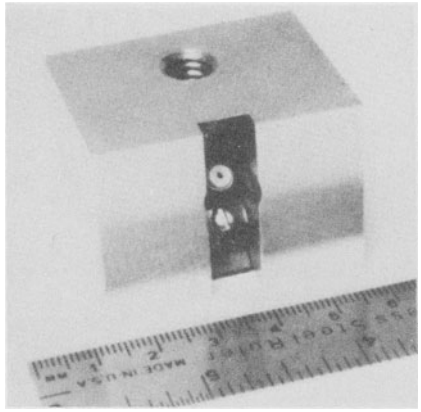

Fig. 1. Transducer in aluminum housing.

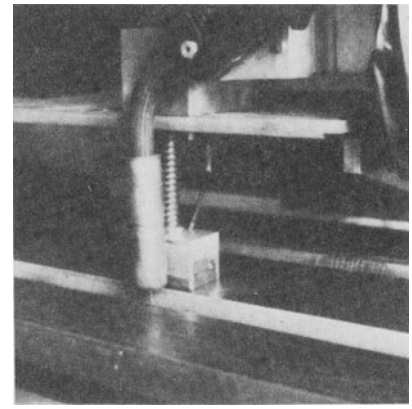

Fig. 2. Transducer fixture aligned with torch.

as small as 0.25 mm. The digitized ultrasonic and position data are stored on a Winchester disk for later reference, backup, and data transfer. The software also performs several control functions during the data acquisition process and stores data about these functions.

GMA Welding

The GMA welding is performed using a Linde side-beam welder and a Cobra-matic wire feed. The welding parameters included currents from 212 to 310 A, voltages from 22 to 28 V, travel speeds from 228.6 to 266.7 mm/min, wire feed rates of 7874 to 12446 mm/min using 1.11 mm feed wire. The average deposition rate is $1.4 \times 10^{-3}$ kg/s (11 lbs/hr). The spray transfer mode is used with a contact-tip-to-work distance of 15.9 mm. The cover gas is 98% argon and 2% oxygen. A weld sample of 25.4 mm thick carbon steel is used with a V-groove bevel having a 60° included angle, a 4.76 mm root opening, and a 6.35 mm backup bar.

Experimental Results

The data presented in this paper are acquired with a stationary transducer mounted on the weld sample with the welding torch moving past the transducer. The stationary transducer data are necessary to determine the optimum alignment of the transducer and the torch and to observe benign geometric reflectors and weld bead geometry reflectors during the entire welding process. Other data, not presented here, are obtained with the transducer moving with the torch.

Figure 4 illustrates the signals present as the torch moves past the transducer. To obtain the greatest amplitude signals, the optimum position of the transducer was determined to be 3 to 5 mm behind the torch tip using the stationary 5 MHz transducer normal to the weld preparation. For the data collected it is observed that the signals from the weld bead vary from weld to weld using the same transducer.

Destructive Evaluation

To resolve the causes of the variation in the signal amplitude and the diversity of signals observed in the acquired A scans, destructive evaluation was performed at each weld area to establish the geometry of the weld bead. In selected areas three weld sections were made every 4.1 mm,

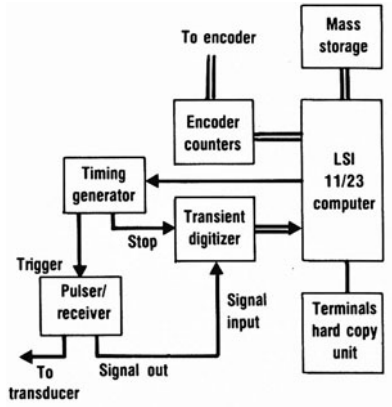


Fig. 3. Computer data acquisition system block diagram.

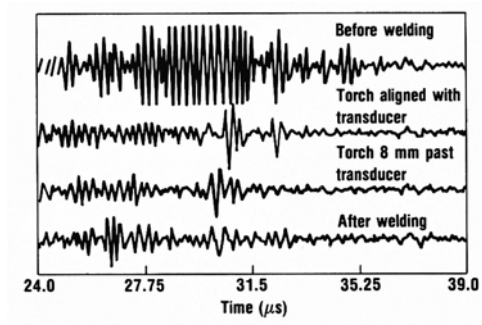


Fig. 4. A-scans from weld pool moving past stationary transducer.

with the middle section at the transducer sound centerline, to determine the variation of weld bead geometry within the beam spread of the transducer. The sectioned, mounted, polished, and etched samples show that the weld bead geometry varies over 12.3 mm (Fig. 5). This may account for the diversity of the signals observed during the stationary transducer data acquisition tests.

## MACHINED SAMPLES

Because of the diversity of the weld bead geometries observed in the destructive evaluation samples, machined samples simulating the weld preparation prior to welding, the molten/solid interface during welding, and the solidified weld bead after welding were made in order to understand the various signals observed during the root pass. These machined samples are able to simulate selected weld bead geometries because the molten/solid interface does not support shear waves and sound reflects at this interface. The four sample geometries selected to represent the geometry

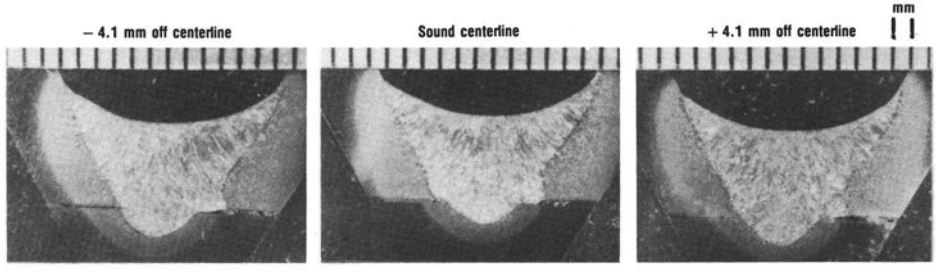


Fig. 5. Polished and etched root weld samples showing variation in weld pool penetration.

during welding are typical of those seen in the destructive samples. Care was taken in the machining directions to assure that a root pass was simulated with a fill level of 7 mm and side wall penetration of no more than 2.5 mm.

Data collection for these samples was done with the broadband 5 MHz transducer positioned 12 mm from the top of the weld preparation (27 mm from the bottom preparation corner prior to machining). Significantly different signals were received from the machined samples when compared to the corner sample (Fig. 6a). The corner sample A scan shows that two reflectors are present. The reflector at 30.3 μs is due to a specular path from a ray with a 60° incident angle and the second at 31 μs is from the bottom corner on a 1/2 vee path from a ray with a 45° incident angle. The specular path signal, confirmed using the ray tracing field code, normally would not be observed during ambient temperature inspection, but, because additional gain is required to overcome the larger attenuation at higher temperatures, this signal can be observed.

In the machined sample in Fig. 6b the main reflector is the new corner, with the signal occurring at 29 μs which is sooner in time than the preparation corner because of the reduced sound path to the new corner. Figure 6c simulates the single radius penetration seen in many samples. The two reflectors, at 28.3 and 29.5 μs, are due to a ray reflected from the curved surface and a ray with a 43° angle of incidence reflected from the new bottom corner, respectively. The simulated weld geometry in Fig. 6d also shows two distinct reflectors. The signal at 28 μs is from the curve of the upper radius and the signal at 28.8 μs is from the new bottom corner. Additional signals are seen after the corner signal in this A scan and are due to bounces inside the part off the curved surfaces. The final sample (Fig. 6e) is similar to the previous sample, but the bottom radius is in convex rather than concave. The corner reflector in this sample is reduced in amplitude because the corner (28.8 μs) is no longer a good geometric reflector. The reflection from the upper radius generates the largest amplitude signal in the A scan, which occurs at 28 μs. Signals that occur later in time than 28.8 μs are also observed in Fig. 6e due to complex bounces in the part.

Figure 6e is a simulation of the weld bead geometry observed by the stationary transducer in Fig. 4 (the second A scan) with the exception that the bottom corner is more rounded; therefore, the B signal (Fig. 6e) is not easily seen in the actual weld A scan. The time between the A signal and the complex bounce signals in Fig. 6e is 2 μs. Since the same time separation is seen between the two signals in the actual weld signal, a good correlation exists between the A scan of the actual weld and the simulated model. It should be noted that the transducer "sees" a dynamic weld bead geometry which can not be simulated easily by a machinist. Still, the correlation between the A scans provides assurance that the digitized and video data provide a chronological record of the dynamic weld bead geometry from formation to solidification.

To determine the reflectors in the solidified weld, samples were also machined to simulate the various fill levels of the solidified weld to determine the benign geometric reflectors that can be detected. Figure 7 is typical of the A scans observed. The signal at 29.7 μs is from the corner and the two signals later in time are from the top of the machined weld surface. The corner signal in Fig. 7 correlates to the forming signal seen at 30 μs in the fourth A scan in Fig. 4.

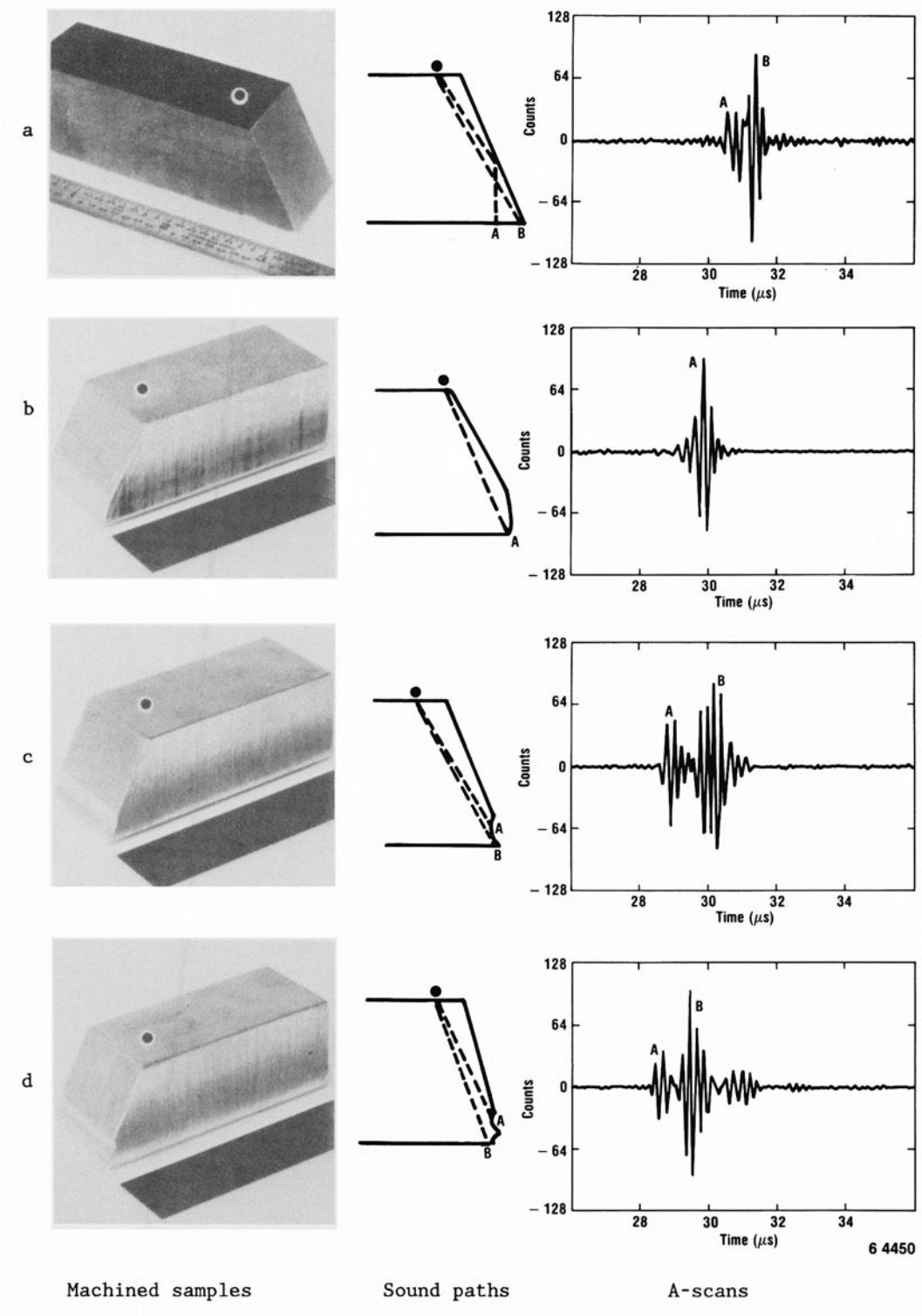


Fig. 6. Machined samples that simulate the solid/liquid interface geometries of a penetrating weld pool and ultrasonic reflections from the interfaces.

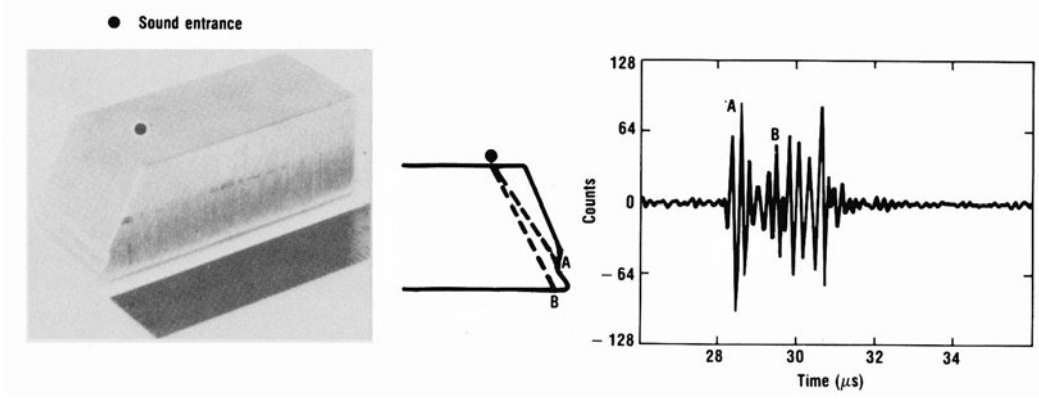


Fig. 6. (Continued)

## CONCLUSION

This research has shown that the molten weld pool can be observed as it is formed using standard transducers and wedges, providing they are shielded from the radiant heat of the welding arc. The formation of the weld bead geometry is a dynamic process that can generate many unique signals within the beam spread of the transducer. With careful analysis of the echoes from machined samples that simulate the corner preparation, weld bead geometry, and solidified weld geometry, the location of significant signals can be determined at ambient temperatures. There appears to be a good correlation between the ambient temperature work and data acquired during actual weld runs. The next step in the research effort is to upgrade the temperature gradient field code and the ray tracing field code to model the current weld sample geometry and transducer sound field in order to validate the location of signals seen during welding. This code will also be used to determine the optimum ultrasonic parameters to use to detect the weld bead geometry for a welding application. If the validation work confirms that the signals observed are from the weld bead geometry, an input signal is present that can provide information about the depth of fill, amount of side wall penetration, and the geometry of the weld bead for the closed-loop welding system.

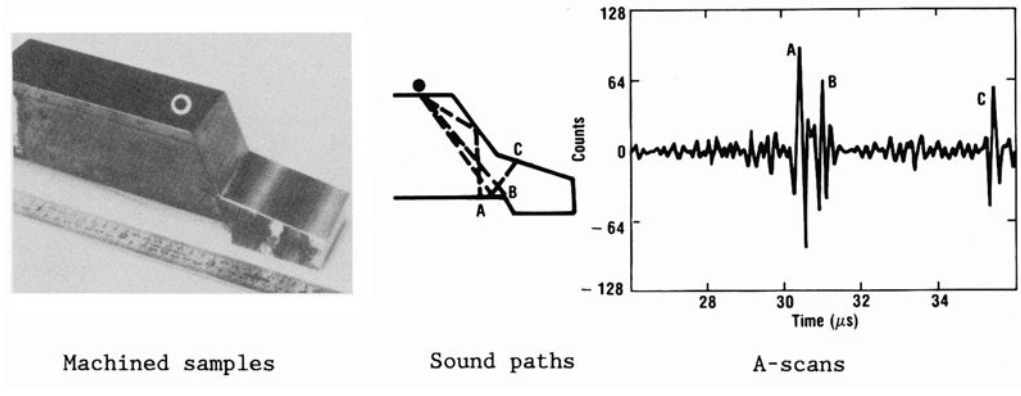


Fig. 7. Machined sample that simulates the solidified weld pool.

ACKNOWLEDGMENTS

This work is supported by the U. S. Department of Energy, Office of Energy Research, Office of Basic Energy Sciences under DOE Contract No. DE-AC07-76ID01570. Appreciation is expressed to U. S. Wallace, G. L. Fletcher, and N. G. Boyce for technical assistance.

REFERENCES

1. J.A. Johnson, N.M. Carlson, J.O. Bolstad, H.B. Smartt, M.B. Ward, R.T. Allemeier, L.A. Lott, and D.C. Kunerth, "Automated Welding Process Sensing and Control," 1986 Proceedings of the Second International Symposium on the Nondestructive Characterization of Materials, to be published in 1986.

2. H.B. Smartt, C.J. Einerson, and A.D. Watkins, "Modelling and Control of Gas Metal Arc Welding," in preparation, to be submitted to Welding Journal.

3. L.A. Lott, J.A. Johnson, and H. B. Smartt, "Real-Time Ultrasonic Sensing of Arc Welding Processes," Proceedings, 1983 Symposium on Nondestructive Evaluation Applications and Materials Processing, pp. 13-22, American Society for Metals, Metals Park, OH.

4. J.A. Johnson and N.M. Carlson, "Weld Energy Reduction by Using Concurrent NDE," NDT International, June 1986.

5. N.M. Carlson and J.A. Johnson, "Ultrasonic Inspection of Partially Completed Welds Using Pattern-Recognition Techniques," Review of Progress in Quantitative Nondestructive Evaluation, 1986, pp.773-780

6. J.A. Johnson, B.A. Barna, L.S. Beller, S.C. Taylor, and J.B. Walter, "A CAMAC Based Ultrasonic Data Acquisition Workstation," submitted to Materials Evaluation.